Spin transport in helical biological systems

Elena Díaz* and Rafael Gutierrez†

*GISC, Departamento de Física de Materiales, Universidad Complutense, E-28040 Madrid, Spain
†Institute for Materials Science, Dresden University of Technology, 01062 Dresden, Germany

Abstract. Motivated by the recent experimental demonstration of spin selective effects in monolayers of double-stranded DNA oligomers, our work presents a minimal model to describe electron transmission through helical fields. Our model highlight that the lack of inversion symmetry due to the chirality of the potential is a key factor which will lead to a high spin-polarization (SP). We also study the stability of the SP against fluctuations of the electronic structure induced by static disorder affecting the on-site energies. In the energy regions where the spin-filtering occurs, our results remain stable against moderate disorders although the SP is slightly reduced.

Keywords: Spin-filtering, DNA-molecules, helical field, Anderson disorder
PACS: 73.22.-f 73.63.-b 72.25.-b 87.14.gk 87.15.Pc

INTRODUCTION

Recent experiments have demonstrated double-stranded DNA molecules as efficient spin filters at room temperature [1, 2]. Generally speaking the spin sensitivity of organic spintronic devices [3, 4, 5] is basically related to two possible issues: the magnetic properties of the organic material or those of the electrodes where the molecules is attached. Therefore this experimental observation was quite surprising due to the low spin-orbit coupling present in the atoms of DNA bases. What makes DNA different in this discussion? Its helical conformation. This geometry presents quite specific symmetry properties and it must be a key ingredient for the theoretical explanation of these experiments [2]. So far there are two different experimental lines. On one hand in Ref. [1] an Au-substrate where the DNA monolayer were deposited is irradiated by light, being the emmitted electrons energy clearly superior to the energy scale of DNA molecular orbitals. Thus, here we will deal with a scattering process [6, 7]. On the other hand experiments of Ref. [2] probe the conductivity of DNA monolayer in a two-terminal setup, namely a quantum transport scenario [8, 9, 10]. In this manuscript we will focus on this second class of experiments by extending the study of the model presented in Ref. [8]. Our main objective is to study how stable the spin-selective effects are against a disordered perturbation of the electronic structure.

MODEL HAMILTONIAN

Our starting point is the discrete Schrödinger equation for a particle moving along the molecular axis direction (z-axis for convenience) of a helical molecular system in the presence of spin-orbit coupling (SOC). We assume the system to be formed by stacking molecular units which give rise to the helical structure, as well as the electrostatic properties of the medium. It can be demonstrated [11] that in the case of a charged helical array the present electric field resembles the helical symmetry. In our case we confine the charge motion to the z-axis and therefore, we only focus on the components of such field at the molecular axis. Under these assumptions the potential and the electric field read:

$$\begin{aligned} U(z) &= U_0 \sum_{l,j} \frac{1}{(a^2+(z-lb-j\Delta z)^{1/2}} \\ \mathbf{E}(z) &= -E_0 \sum_{l,j} g_{l,j}(z)(\cos(Qj\Delta z), \sin(Qj\Delta z)). \end{aligned} \tag{1}$$

Here, $g_{l,j}(z) = (1+[(z-lb-j\Delta z)/a]^2)^{-3/2}$, and $Q = 2\pi/b$, with b being the helix pitch and a the helix radius, see Fig. 1. The index $j = 0, \cdots, M-1$ runs along one helical turn and labels the z-coordinate of the M molecular units placed along one turn of the helix. The index $l = -L/2, \cdots, L/2$ (L being the number of helical turns) connects sites which differ in their z-coordinate by b. More importantly the factor E_0 is proportional to the local charge density.

15th International Conference on Transport in Interacting Disordered Systems (TIDS15)
AIP Conf. Proc. 1610, 141-146 (2014); doi: 10.1063/1.4893525

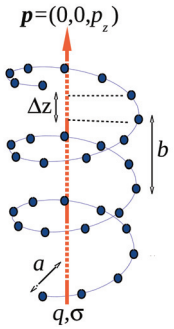

FIGURE 1. The charge q in spin state σ is moving with momentum p_z along the molecular axis (chosen as the z-axis hereafter). The charge motion takes place under the effect of the SOC induced by the electric field created by a helical charge array. The parameters a, b and Δz are the radius and the pitch of the helix and the spacing of the z-component of the position vector of the charges distributed along it, respectively.

The effect of the field $\mathbf{E}$ on a charge moving with momentum $\mathbf{p} = (p_x, p_y, p_z)$ induces a magnetic field in the charge's rest frame, leading to a SOC: $H_{SO} = \lambda\sigma(\mathbf{p} \times \mathbf{E})$. The SOC strength is $\lambda = e\hbar/(2mc)^2$ and σ is a vector whose components are the Pauli matrices σ_x, σ_y, σ_z. Although the electric field is calculated by the three dimensional (3D) helical charge distribution, the linear particle motion reduces the study to a one-dimensional (1D) problem. Due to the spin degree of freedom, the problem can be written as an effective 2-legs tight-binding model, where each leg corresponds to a given spinor component ($\uparrow$ and $\downarrow$) as follows (see Ref.[8] for the complete derivation):

$$\begin{aligned} H &= \sum_{\sigma=\uparrow,\downarrow}\sum_{n=1}^{N} U_n c^{\dagger}_{n,\sigma} c_{n,\sigma} + V \sum_{\sigma=\uparrow,\downarrow}\sum_{n=1}^{N-1} (c^{\dagger}_{n,\sigma} c_{n+1,\sigma} + \text{h.c.}) \\ &+ \sum_{n,m=1}^{N} (c^{\dagger}_{n,\uparrow} W_{n,m} c_{m,\downarrow} + c^{\dagger}_{m,\downarrow} W^{\times}_{m,n} c_{n,\uparrow}) + H_{leads}. \end{aligned} \tag{2}$$

The operators $\{c_{n,\sigma}, c^{\dagger}_{n,\sigma}\}_{n=1,\ldots,N,\sigma=\uparrow,\downarrow}$ create or destroy, respectively, an excitation at the tight-binding site n with spin index σ. The only non-zero elements of the inter-channel coupling matrix $\mathbf{W}$ are given by: $W_{n,n} = -\alpha f(n\Delta z)$, $W_{n,n+1} = \alpha\Psi(n\Delta z)/2\Delta z$, and $W_{n+1,n} = -\alpha\Psi((n+1)\Delta z)/2\Delta z$. Further, the matrix $W^{\times}_{n,m}$ satisfies $W^{\times}_{n,m} = -(W_{m,n})^*$ for $n \neq m$, and $W^{\times}_{n,n} = (W_{n,n})^*$, which reflects time inversion symmetry in the system. The hopping V can be estimated via a first-principle calculation of the electronic structure for a given system and U_n is evaluated according to Eq. 1. Finally, the operator H_{leads}, considered within the Landauer-Büttiker formalism, includes the coupling to the electrodes attached to the left and right edges of the SO active region [8].

Transport Description

Spin-dependent transport in the ladder model of the previous section will be represented hereafter as coherent charge transport in the 2-legs Hamiltonian Eq. 2. It is clear that the specific transport mechanism will in general depend on the molecular system and also be influenced by the environmental conditions, e.g. single molecule vs. molecule embedded in a self-assembled monolayer or dry vs. solvent conditions. Being aware of its potential limitations, we will consider transport in the context of the Landauer approach, which provides a simple framework to analyze the influence of different parameters on the spin polarization. We are interested in exploring the possibility of inducing a spin polarization without the need of decoherence as a key element, so that we limit ourselves to compute the zero-bias transmission function $T(E)$ (linear conductance) for our model.

Along similar lines as in Ref. [8], we focus on the spin-dependent transmission probability, $T(E)$, of the model given by Eq. 2, as a function of the electron's injection energy E. The problem can be considered as a scattering problem where a finite-size region (with non-vanishing SOC) is coupled to two independent L(left)- and two independent R(right)-electrodes, each electrode standing for a spin channel and being represented by a semi-infinite chain. $T(E)$ encodes the influence of multiple scattering events in the SOC region. We assume a coherent transport regime and use

Landauer's theory [12] to obtain:

$$\begin{aligned} T(E) &= \Gamma^R_\uparrow(\Gamma^L_\uparrow|G_{1\uparrow,N\uparrow}|^2+\Gamma^L_\downarrow|G_{1\downarrow,N\uparrow}|^2) \\ &+ \Gamma^R_\downarrow(\Gamma^L_\uparrow|G_{1\uparrow,N\downarrow}|^2+\Gamma^L_\downarrow|G_{1\downarrow,N\downarrow}|^2) \\ &= t_{up}(E)+t_{down}(E)\ . \end{aligned} \tag{3}$$

In Eq. 3, $G_{n\sigma,m\nu}(E)$ are matrix elements of the retarded Green's function of the SOC region including the influence of the L- and R-electrodes and $\Gamma^{\mathrm{R,L}}_{\uparrow,\downarrow}$ are the nonvanishing elements of the spectral functions of the left and right electrodes. Notice that we focus on the case where the spectral density matrix Γ^{L} have only non-vanishing elements when coupling the sites 1 of the up and down spin channels, respectively. Similarly, Γ^{R} has only non-zero elements when coupling sites N of the up and down spin channels, respectively. Accordingly and for simplicity the non-vanishing terms in the coupling matrices are abbreviated as follows: $\Gamma^{\mathrm{L}}_{1\uparrow,1\uparrow}=\Gamma^{\mathrm{L}}_\uparrow, \Gamma^{\mathrm{L}}_{1\downarrow,1\downarrow}=\Gamma^{\mathrm{L}}_\downarrow, \Gamma^{\mathrm{R}}_{N\uparrow,N\uparrow}=\Gamma^{\mathrm{R}}_\uparrow$ and $\Gamma^{\mathrm{R}}_{N\downarrow,N\downarrow}=\Gamma^{\mathrm{R}}_\downarrow$

The transmissions for the up and down channels, $t_{up}(E)$ and $t_{down}(E)$, contain contributions arising both from direct transmission without spin-flip as well as spin-flip. An energy-resolved spin-polarization (SP) for different initial spinor states can be defined as:

$$P(E) = (t_{up}(E) - t_{down}(E))/T(E). \tag{4}$$

The energy-average SP $\langle P(E)\rangle_E = P(\langle t_{up}(E)\rangle, \langle t_{down}(E)\rangle, \langle T(E)\rangle)$ will also be used. For the sake of simplicity we focus in general on electron-like contributions ($E<0$) and on energies $|E| \geq k_BT \approx 23$ meV, so that $\langle\ldots\rangle_E = \int_{-2V}^{-k_BT} dE(\ldots)$.

NUMERICAL RESULTS

A crucial parameter in the model is the SOC coupling α. Realistic values are obviously very difficult to obtain [13, 14], since α is not simply the atomic SOC, but contains the influence of the charge distribution in the system via the field factor E_0. In the present work we are going to use similar values, than those estimated in Ref.[8], being aware that a more accurate estimation would require a separate first-principle study of the electronic molecular structure. On the other hand the hopping V in DNA is estimated via a first-principle calculations to lie in the range of few tens of meV [15, 16]. Notice that for the effect under consideration in Ref.[8] it was shown that weak electronic coupling along the helical structure is expected to lead to low mobility of the electrons and to allow enough time for the SOC, although being weak, to influence spin transport. Last, to model the different initial spinor states used in the following, the energy bands of the electrodes can be shifted appropriately. Thus, states of injected electrons polarized with their spin pointing up (P_{10}) or down (P_{01}) can be modeled by strongly shifting the spectra of the electrode corresponding to the spin component $\downarrow$ or spin $\uparrow$, respectively, so that either $\Gamma^L_\downarrow(E)$ or $\Gamma^L_\uparrow(E)$ vanishes within the spectral support $[-2V, 2V]$ of $T(E)$. For the initial unpolarized state (P_{11}) the energy bands of both electrodes are considered identical. In summary, the following sets of couplings are used:

$$\begin{aligned} (10) &\rightarrow \Gamma^{L,R}_\uparrow(E) = \Gamma^R_\downarrow(E), \Gamma^L_\downarrow(E) = 0, \\ (01) &\rightarrow \Gamma^{L,R}_\downarrow(E) = \Gamma^R_\uparrow(E), \Gamma^L_\uparrow(E) = 0, \\ (11) &\rightarrow \Gamma^{L,R}_\uparrow(E) = \Gamma^{L,R}_\downarrow(E). \end{aligned}$$

Effect of the helical symmetry

Energy dependence of the SP for injected electrons with polarization state P_{11} and for two different geometries to clarify the influence of the helical symmetry is shown in Fig. 2. Solid black line corresponds to DNA molecule geometry with pitch b=3.2 nm, as that used in the rest of the manuscript, and dashed green line with b=30.0 nm corresponds to the limiting case where the helical structure of the potential has been almost removed. In the former situation a spin-filter effect takes place for energies near the band edges, where the SP exceeds P_{11} ≈50%. Notice also that near the band edges the SP has opposite signs for electrons ($E<0$) and holes ($E>0$), though $P(E)$ is not exactly antisymmetric. On the other hand, we find that with increasing b the polarization becomes "trivial", i.e. it takes a value

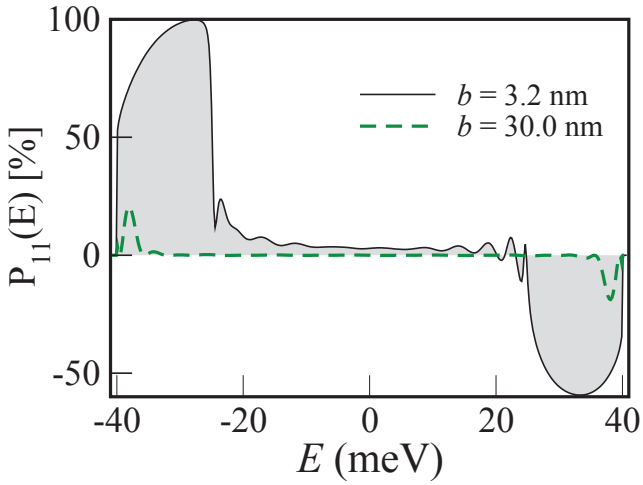

FIGURE 2. Energy dependence of the SP P(E) for L=3 helical turns, and for injected electrons with unpolarized spin state (P_{11}). Parameters: α=4 meV nm, V=20 meV and U_0=5 meV.

of 0% for all energies excepts in a very small region at the band edges. The latter behavior is related to finite-size effects and will dissapear for a finest sampling of the simulations. This happens, since according to the definition of $P(E) = (t_{up}(E) - t_{down}(E))/T(E)$ the case $b \to \infty$ gives $t_{up} = 1$ and $t_{down} = 1$, so that formally $P(E) \to \pm 0\%$ for all energies. This behavior is however irrelevant and only indicates that each incoming spin state is transmitted with no effect of the SOC coupling. Hence, in the frame of this minimal model, the helical structure of the electric field turns out to be a fundamental ingredient in generating the spin filter effect.

In Figure 3, the quantities $\xi_{\rm up} = T_{\uparrow\uparrow} - T_{\downarrow\uparrow}$ and $\xi_{\rm down} = T_{\downarrow\downarrow} - T_{\uparrow\downarrow}$ are plotted for the same geometries as Fig. 2 in order to illustrate the relative amount of spin-conserving and spin-flip processes in the outgoing spin-up and spin-down channels. Notice that, according to the former definitions, if ξ_σ is positive, spin-conserving processes are dominating, while if ξ_σ negative, spin-flip events dominate. Furthermore the insets of Figure 3 show the total transmission of each spin component, keeping in mind that the difference between the curves of $t_{\rm up}$ and $t_{\rm down}$ is proportional to the spin polarization. For the DNA structure (b=3.2 nm), leading to net spin polarization at the band edges, a large degree of spin-flip is found over most of the probed energies. However, it is only at the energies regions where the nonzero SP arises where the magnitudes of $\xi_{\rm up}$ and $\xi_{\rm down}$ are different. In particular at the bottom of the band, the spin-filtering effect mainly results from spin-flip processes while at the top of the band it is related to spin-conserving ones. In both cases, these effects strongly depends on the spin component. On the contrary, when the helical structure dissapears (b=30.0 nm), although spin-flip still dominate against spin-conserving processes, the spin-flip rate of components up and down are basically the same. Therefore, after propagation the state is still unpolarized and the spin polarization vanishes.

Effect of static disorder

In order to test the stability of the spin polarization against fluctuations of the electronic structure induced by static disorder, we have assumed that the site energies are random variables with a square box distribution of width $\Delta\varepsilon$. In Fig. 4 the results obtained by performing a configuration average over 150 realizations of the disorder are shown for $\Delta\varepsilon$=10 meV and $\Delta\varepsilon$=20 meV. The spin polarization turns out to be stronger affected at low energies, while the suppression near $\pm 2V$ is less strong. We remark that the spin filter effect $-$equal sign of the polarization for all incoming states (10), (01), and (11)$-$ occurs mainly near the band edges and hence it is the influence of the disorder within such energy region what is relevant. This behavior does not depend of the strength of the SOC, see inset of Fig. 4. The obtained results thus show their stability against a perturbation of the electronic structure. Clearly, with increasing disorder the spin polarization will be ultimately reduced and eventually suppressed. In summary, if the disorder is not so strong so as to make a coherent transport model based on extended states questionable, the obtained

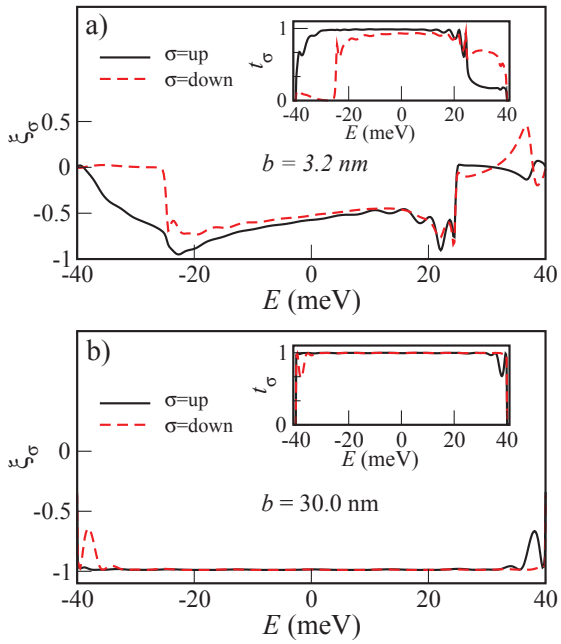

FIGURE 3. Energy-resolved ratios of the transmission function for the outgoing spin-up channel, $\xi_{\rm up} = T_{\uparrow\uparrow} - T_{\downarrow\uparrow}$, and spin-down channel, $\xi_{\rm down} = T_{\downarrow\downarrow} - T_{\uparrow\downarrow}$. Insets show the total transmission $t_{\rm up} = T_{\uparrow\uparrow} + T_{\downarrow\uparrow}$ and $t_{\rm down} = T_{\downarrow\downarrow} + T_{\uparrow\downarrow}$, respectively. The calculations have been performed f

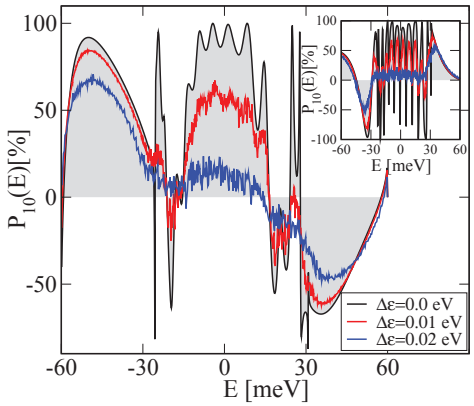

FIGURE 4. Disorder averaged SP for the (10) incoming state and different magnitudes of disorder $\Delta\varepsilon$ for the same parameters of the upper panel of Fig. 2. Inset shows same as main plot for $\alpha = 6$ meV nm.

spin polarization is only reduced but not fully suppressed.

CONCLUSIONS

In this work we have considered a 1D coherent spin transport model to study the main theoretical ingredients to reveal the spin filtering effect observed in double-stranded DNA molecules. We have demonstrated that the chiral symmetry of such molecules, which we included by way of a helical electric field, gives rise to a relevant SOC effect and thus, to a finite spin-polarization in the system. Furthermore we have identified that within this model the spin filtering effect

mainly results from an interplay between spin-flip and spin conserving proccesses that strongly depend on the spin state and on the propagation energy.

Our results remain stable against moderate disordered fluctuations. However, for disorder strengths $\Delta\varepsilon \sim V$ or larger, localization effects will dominate the physics and the microscopic transport mechanism will also change, so that a different model as that presented in the current study should be used. For example, decoherence to mimic hopping transport can be introduced via Büttiker probes [17] or by directly formulating the problem in terms of master equations. It worths noticing however that the experimental systems studied so far are self-assembled monolayers (SAM) of DNA or other chiral molecules. In this case, we may safely expect that conformational disorder will in general strongly quenched, first due to steric hindrance and second to the attachment of the molecules to a substrate. This situation is in clear contrast to cases where molecules are studied in the gas phase or single molecules on substrates. In these two latter cases, disorder may play a considerably more important role; however, due to the lacking of corresponding experiments addressing spin polarized transport in single chiral molecules, a conclusive statement can not be provided.

ACKNOWLEDGMENTS

This work was supported by the Ministerio de Economia y Comptetitividad (MINECO) project PRI-AIBDE-2011-0927 and by the German Academic Exchange Service (DAAD) project 54367888 within the joint program *Acciones Integradas*. Computational resources were provided by the ZIH at TU-Dresden. E.D was further supported by MINECO project MAT 2010-17180. R.G. acknowledges support from the German Excellence Initiative: Cluster of Excellence EXC 1056 "Center for Advancing Electronics Dresden" (cfAED).

REFERENCES

1. B. Goehler, V. Hamelbeck, T. Z. Markus, M. Kettner, G. F. Hanne, Z. Vager, R. Naaman, and H. Zacharias, *Science* **331**, 894–897 (2011).
2. Z. Xie, T. Z. Markus, S. R. Cohen, Z. Vager, R. Gutierrez, and R. Naaman, *Nano Letters* **11**, 4652–4655 (2011).
3. Z. H. Xiong, D. Wu, Z. Valy Vardeny and J. Shi, *Nature* **427**, 821–824 (2004).
4. K. S. Li, *et al.*, *Phys. Rev. B* **83**, 172404–1–172404–4 (2011).
5. D. Sun *et al.*, *Phys. Rev. Lett.* **104**,236602–1–236602–4 (2010).
6. S. Yeganeh, M. A. Ratner, E. Medina and V. Mújica, *J. Chem. Phys.* **131**, 014707–1–014707–9 (2009)
7. E. Medina, F. López, M. Ratner, V. Mújica, *European Phys. Lett.* **99** 17006–p1–17006–p5 (2012)
8. R. Gutierrez, E. Díaz, R. Naaman, G. Cuniberti, *Phys. Rev. B* **85**, 081404(R)–1–081404(R)–4 (2012)
9. A. M. Guo and Q. F. Sun, *Phys. Rev. Lett.* **108**, 218102–1–218102–4 (2012)
10. R. Gutierrez, E. Díaz, C. Gaul, T. Brumme, F. Domínguez-Adame, and G. Cuniberti, *J. Phys. Chem. C* **117**, 22276–22284 (2013)
11. D. Hochberg, G. Edwards, and Th. W. Kephart, *Phys. Rev. E* **55**, 3765– (1997).
12. A. Nitzan, Annu. *Rev. Phys. Chem.* **52**, 681– (2001).
13. C. L. Kane, E. J. Mele, *Phys. Rev. Lett.* **95**, 226801–p1–226801–p4 (2005).
14. Z. G. Yu, *Phys. Rev. Lett.* **106**, 106602–p1–106602–p4 (2011).
15. P. B. Woiczikowski, T. Kubar, R. Gutierrez, G. Cuniberti, and M. Elstner, *J. Chem. Phys.* **130**, 215104 (2009).
16. R. Gutierrez, R. A. Caetano, B. P. Woiczikowski, T. Kubar, M. Elstner, and G. Cuniberti, *Phys. Rev. Lett.* **102**, 208102–p1–208102–p4 (2009).
17. D. Nozaki,C. G. da Rocha, H. M. Pastawski, G. Cuniberti, *Phys. Rev. B* **8**, 155327–p1–155327–p6 (2012).